

CONTRACT NUMBER 508830

DEISA
**DISTRIBUTED EUROPEAN INFRASTRUCTURE FOR
SUPERCOMPUTING APPLICATIONS**

European Community Sixth Framework Programme
RESEARCH INFRASTRUCTURES
Integrated Infrastructure Initiative

Production operation of distributed simulation codes: status
report — second set of projects

Deliverable ID: DEISA-D-JRA6-7

Due date: April 30th, 2007

Actual delivery date: May 25th, 2007

Lead contractor for this deliverable: IDRIS / CNRS, France

Project start date: May 1st, 2004

Duration: 4 years

Project co-funded by the European Commission within the Sixth Framework Programme (2002-2006)		
Dissemination Level		
PU	Public	X
PP	Restricted to other programme participants (including the Commission Services)	
RE	Restricted to a group specified by the consortium (including the Commission	
CO	Confidential, only for members of the consortium (including the Commission Services)	

Table of Content

Table of Content.....	1
1. Introduction.....	2
1.1 Executive Summary.....	2
2. Natural convection / radiation project	3
2.1 Coupled 2D numerical simulations.....	3
2.1.1 Building the numerical simulation.....	3
2.1.2 Comparison with experiment.....	4
2.2 3D coupled application	4
2.2.1 Technical 3D coupling improvements.....	4
2.2.2 Numerical model enhancements.....	5
2.2.3 Results of first coupled calculations	5
2.2.4 Conclusion of the 3D natural convection / radiation coupling project	8
2.3 Conclusion.....	8
3. FOCUS project	9
3.1 Using PALM technology	9
3.1.1 Overview.....	9
3.1.2 Implementing PALM technology.....	9
3.1.3 Deployment on the DEISA infrastructure.....	10
3.1.4 Conclusion.....	10
3.2 DECI simulations — numerical results	11
3.2.1 Gas turbine simulation.....	11
3.2.2 Diedra simulation.....	11
3.3 Conclusion and future work.....	15
4. The KOP3D project.....	17
4.1 Current Scientific Usage and Improvements	17
4.2 Reduction of Coupling Loads	17
4.3 Heterogeneous Parallelism	18
4.4 Improvements on Load Balancing.....	20
4.5 Conclusions.....	22
5. New projects	24
5.1 Fluid / structure coupling (BACI).....	24
5.1.1 Scientific project	24
5.1.2 Objectives in this Joint Research Activity	24
5.2 Molecular Dynamics / Visualisation project	24
5.2.1 Scientific project	24
5.2.2 Objectives in this Joint Research Activity	25
5.3 Quantum Mechanics / Molecular Mechanics project	25
5.3.1 Scientific project	25
5.3.2 Objectives in this Joint Research Activity	26
6. Conclusion.....	27
7. References and Applicable Documents.....	28
8. Document Amendment Procedure	30
9. List of Acronyms and Abbreviations	31

1. Introduction

1.1 *Executive Summary*

The main objectives of this activity is to facilitate scientific research projects based on coupling methodology and to provide efficient solutions to exploit these complex applications on the DEISA infrastructure.

The JRA6 activity started with three coupling projects called the *first set* which have been reported in the D-JRA6-1 [12], D-JRA6-2 [13] and D-JRA6-3 [14] deliverables.

This first step was followed by a *second set* of projects of which the scientific projects and the main objectives were described in the D-JRA6-4 [15] deliverable. After porting the three coupled applications on the DEISA infrastructure (see D-JRA6-4 [15]), several important enhancements were operate and the new releases were exploited (see D-JRA6-5 [16]) in DEISA context.

This reporting period concerns the end of the projects of the *second set*. After describing the last improvements, for each project we comment about the last numerical simulations and, to conclude, we highlight the added value on the scientific and technical aspects in this JRA context.

We terminate this document by describing the scientific and technical objectives of the three following projects of the *third set*.

This document is public.

2. Natural convection / radiation project

<i>Title</i>	Coupling of turbulent natural convection with radiative heat transfer in buildings
<i>Scientific leader</i>	Shihe XIN, LIMSI-CNRS (Laboratoire d'Informatique pour la Mécanique et les Sciences de l'Ingénieur), Orsay, France.
<i>Partner Laboratories</i>	LET (Laboratoire d'Etudes Thermiques), Poitiers, France. EM2C (Laboratoire d'Energetique Moléculaire et Mascroscopique, Combustion), <i>Radiative Transfer team</i> , Chatenay Malabry, France.
<i>Links with other scientific projects</i>	COCORAPHA (COuplage CONvection-RAYonnement Pour l'HABitat) - ACI Energie (Action Concertée Initiative) – funded by the French Ministry of Research.

In the previous deliverables [15] and [16], we highlighted the need to take into account radiative heat transfer to describe the fluid behavior inside a 2D square cavity filled with air. Next, we are going to describe the current status of the last coupled application release, the last 2D numerical results and the first 3D numerical results.

2.1 Coupled 2D numerical simulations

The last six months, we took advantage of experiments led by the LET laboratory to compare them to our numerical simulations. Briefly, the experimental set-up consists of a cubic cavity of 1 meter height (L_{ref}) filled with a medium composed by 20 % of carbon dioxide and air (see [27]). The temperature difference between the 2 isothermal walls is set to 15 K and induces a Rayleigh number $R_a = 1.8 \times 10^9$. The wall radiative properties correspond to an 0.2 emissivity value (ϵ) of 0.2.

2.1.1 Building the numerical simulation

A preliminary study has been led by the LIMSI laboratory to calibrate the numerical model at high Rayleigh number. For this study a 1 meter height cavity (L_{ref}) with a 0.5 emissivity value (ϵ) for the cavity walls and a 1 m^{-1} absorption coefficient (κ) of the air inside the cavity have been considered.

The coupled application was numerically configured in adequacy with the physics studied. In particular, we paid attention to avoid inessential computations.

- A specific study had shown that, for this configuration, the results are not sensitive to scheme order higher than 8 for the quadrature sets used by the Discrete Ordinate Model (DOM). An 8-order quadrature scheme is sufficient and has been taken for next simulations.
- Since we need to correctly represent the velocity gradient along vertical walls at high Rayleigh number, a high spatial resolution (400x400 cells) has been chosen.
- Based on studies reported in the previous deliverable [16], the coupling frequency has been estimated for 2 emissivity intervals ($f = 150$ time step for $0.1 \leq \epsilon \leq 0.7$ and $f = 50$ time step for $0.7 \leq \epsilon \leq 0.9$).

Numerical results obtained with this configuration confirm the good behavior of the coupled application. As expected, increasing L_{ref} and/or ϵ leads to increase the thermal transfers between isothermal walls. The vertical velocity at half-cavity height and the

horizontal velocity at half-cavity width increase too (in absolute value) and extreme values turn out to be closer to walls.

2.1.2 Comparison with experiment

At first, several absorption coefficient values ($\kappa = 0, 1, 2, 5 \text{ m}^{-1}$) have been investigated and compared to results obtained with experiment.

A change in the gas dynamics has been observed when increasing the absorption coefficient: horizontal velocity near top wall increases and gets closer to the wall (see Figure 1) and vertical velocity tends to slightly spread out towards the cavity center (see Figure 1).

A relatively good agreement between experimental and numerical results is obtained in particular for $\kappa = 1 \text{ m}^{-1}$. The disagreement of numerical results for $\kappa = 0 \text{ m}^{-1}$ (without participating medium) with experiment ones (see Figure 1), demonstrates again that it is essential to take into account the Radiative Heat Transfers in the medium.

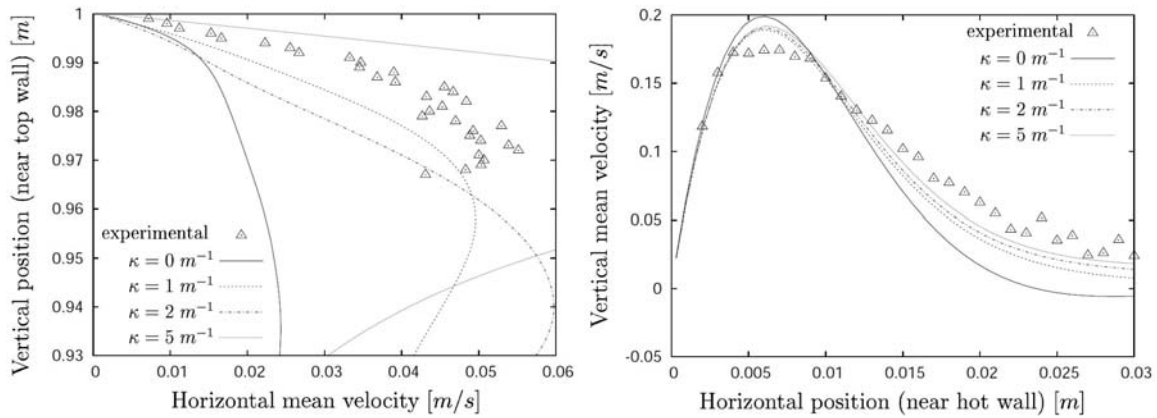


Figure 1: Comparison between experimental and numerical mean velocities in wall vicinity with a medium composed by 20% carbon dioxide and air. Horizontal mean velocity near top of wall is represented in (a) and vertical mean velocity near hot wall at half-cavity height is shown in (b).

Exploring different 2D physical configurations tends to validate the coupled approach and provides realistic simulations of convection in air-filled cavity and seems to give useful information to investigate the more CPU time consuming 3D simulations. Nevertheless, future numerical simulations should consider a better gas model (such as the Spectral-Line Weighted-sum-of-gray-gases, also referenced SLW method) in order to obtain more accurate numerical results.

2.2 3D coupled application

2.2.1 Technical 3D coupling improvements

Concerning the coupling interface, we implemented the asynchronism mechanisms on the client part. This new feature avoids NS3D code to wait the end of the radiative field computation of the RadMC3D code. At the same time, we optimized the coupling part by providing a better overlapping between the 2 coupled codes.

Previously, the 2D case studies have confirmed that the two codes do not need to exchange data in every Navier-Stokes iteration. Nevertheless the update rate or coupling frequency must be adjusted in adequacy with the physical configuration and in particular with the Rayleigh number. This functionality has been added to the 3D code release.

Timing utilities have also been added to help us to adjust the number of processors for each coupled code (RadMC3D and NS3D) to have a better load balancing of the two codes. The time sampling has been set before and after the CORBA invocations and services in the adapter layer.

These new enhancements allow deploying the coupled application on much more processors than the preceding release. The first small numerical simulations show a very good use of the processors. Up to 91 % of the 64 processors are used for a coarse load-balancing adjustment.

2.2.2 Numerical model enhancements

As mentioned in the previous deliverable [16], the first release of the 3D coupled application was ready to run and the first calculations were launched.

The first results outlined some issues and one major problem was identified: for the first launched simulations we checked the program for well-known configurations with a low Rayleigh (Ra) dimensionless number of 10^5 . With this configuration and a 1-meter reference length, the resulting temperature difference was about 10^{-3} K. But the coupled application response was very surprising and showed that the radiation Monte Carlo calculation with about $5 \cdot 10^7$ photon bundles was far from convergence. In fact, for very small temperature differences, the Monte Carlo Method (MCM) required a huge number of statistical events to calculate small differences between local absorbed and emitted energies in these quasi-thermal equilibrium situations. An original solution was developed to overcome this convergence difficulty. Using the superposition theorem applied to the radiative transfer equation, the radiation intensity was split into an equilibrium part at the mean temperature level, and a perturbation term calculated through MCM. This resulted in a reduction of many orders of magnitude in MCM computational times.

So, after the implementation of this superposition and an improvement of the interpolation, the 3D coupled synchronous application was ready.

Many configurations were tested with changing parameters such as the number of processors, the spatial scale in each code or the refinement between the two meshes. As the CPU time for the radiation part is much higher than the one for the convective part at each iteration, we have studied the suitable balance between the number of processors allocated to each calculation, and the appropriate frequency of radiation calculations. Indeed, while convective calculations require relatively small time steps for convergence criteria, it is not necessary to calculate the radiation field at each time step.

2.2.3 Results of first coupled calculations

For these simulations we consider a 1-meter length cubic cavity with two face-to-face vertical walls maintained at fixed temperatures. The temperature difference imposes the Ra number. The other walls are assumed to be adiabatic. The 3D Navier-Stokes equations are solved using *Wang et al.*'s approach [23].

In the case of pure natural convection we assume that the working fluid (air) is a transparent gas and that the radiative flux is equal to zero at the boundaries. When we take radiation into account we assume the same emissivity, $\epsilon=1$, on each wall and the studied cavity is filled with air of which CO_2 and H_2O molar concentrations are respectively fixed at 1% and 3%.

The two models common characteristics are Ra ($3 \cdot 10^7$), the Prandtl dimensionless number Pr (0.707), the average temperature T_0 (300 K), the reference length L_{ref} (1 m), the thermal diffusivity of air a ($2.25 \cdot 10^{-5}$ m²/s) and the thermal conductivity of air λ ($2.63 \cdot 10^{-2}$ W/(m.K)). It is worth of notice that radiation acts not only as an additional source

term in the energy equation, but it also participates as an additional radiative flux in thermal boundary conditions.

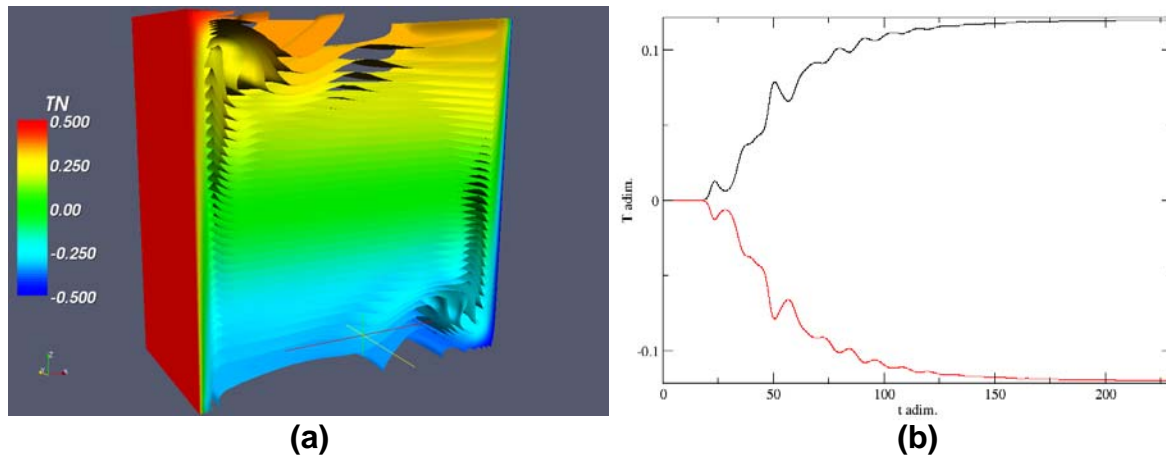


Figure 2: Instantaneous temperatures field without radiation in the $y=0.5$ plane (a) (hot wall on the left and cold wall on the right) and (b) temporal temperature evolution for two points (black: $(0.5, 0.5, 0.625)$, red: $(0.5, 0.5, 0.375)$).

As we can see on Figure 2-a, and according to previous 2D calculations, the 3D-Navier-Stokes results in the median plane ($y=0.5$) are very close to the 2D ones. This is confirmed with the value of the Y velocity component which is very close to 0. But this situation disappears when we approach the walls and especially the corners of the cavity. Moreover, according to the temporal temperature evolution we can notice that we reach a steady state, as already found by other researchers for this Ra value.

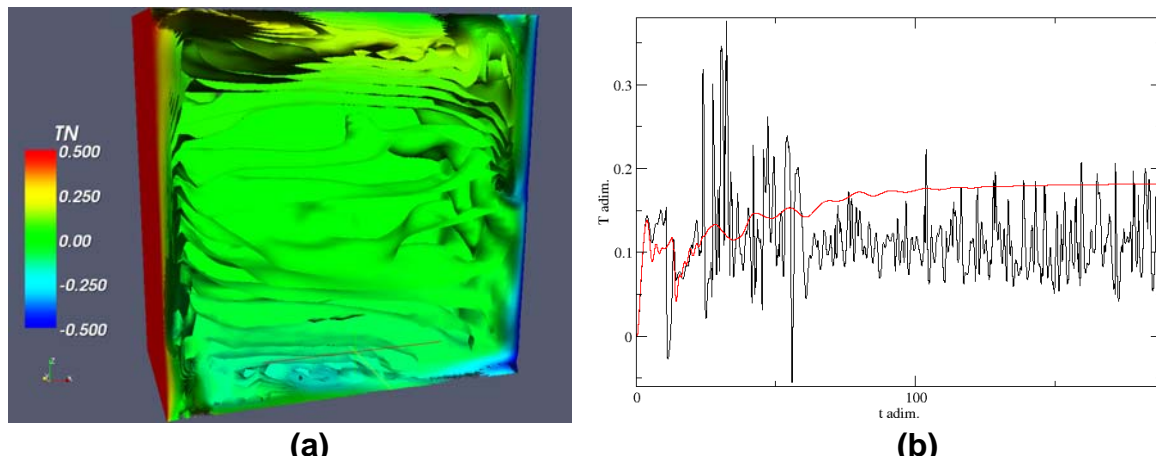


Figure 3: Instantaneous temperature field with radiation in the $y=0.5$ plan (a) (hot wall on the left and cold wall on the right) and (b) temporal temperature evolution with radiation (black) and without radiation (red) at a same point $(0.04, 0.5, 0.76)$.

If we compare Figure 2-a and Figure 3-a, we can notice that the structure of the temperature field is different with or without radiation. In fact, radiative effects break the centre symmetry that we have observed in the pure natural convection case. Moreover, the comparison of the temporal temperature evolution between the two cases at the same position (Figure 3-b) shows that we do not have a steady state with the radiative configuration. Indeed, the application of a Fast Fourier Transform on our temporal signal did not make appear a clear frequency. It means that we have a chaotic system when radiation is taken into account. Let notice also that the structure of the temperature field

near the adiabatic top and bottom walls is deeply modified due to radiative fluxes at the walls.

To complete these comparisons, we present in Figure 4 some consecutive temperature fields spaced with a 0.2 dimensionless time step. We can observe on this figure the destabilization of the boundary layers and the unsteady behaviour of the flow.

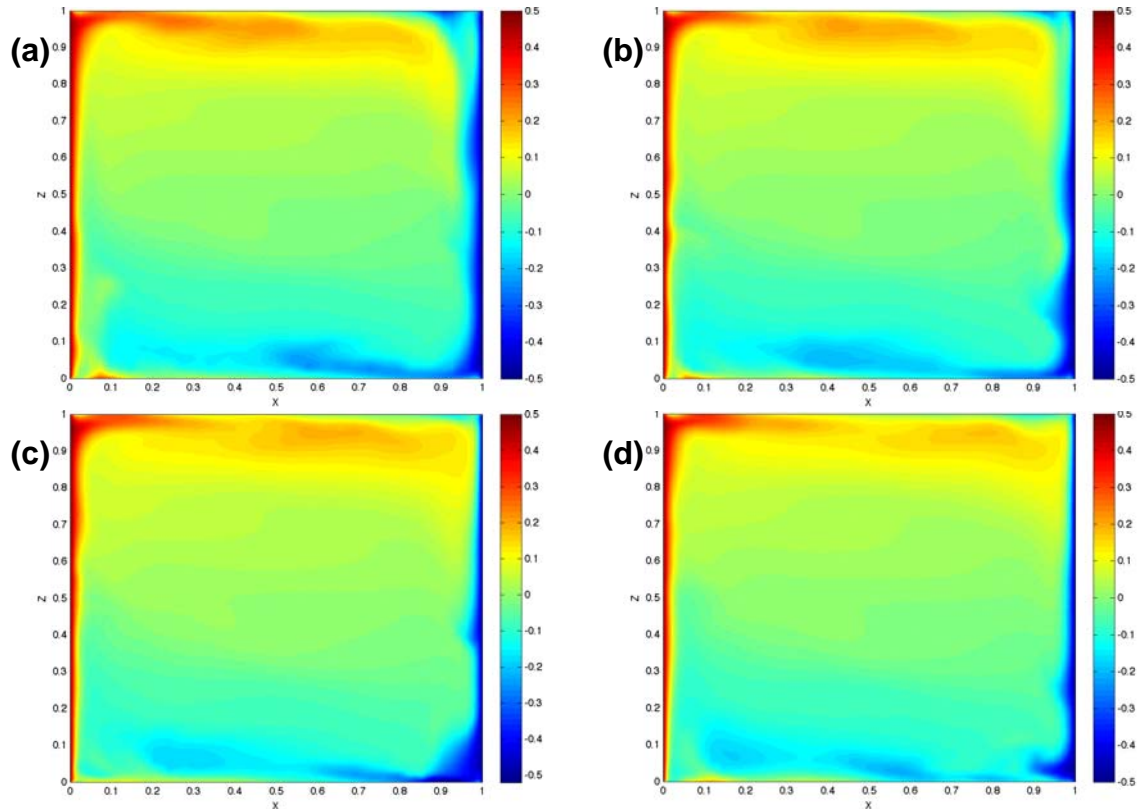


Figure 4: Instantaneous temperatures fields with radiation in the $y=0.5$ plane (spaced with a 0.2 dimensionless time).

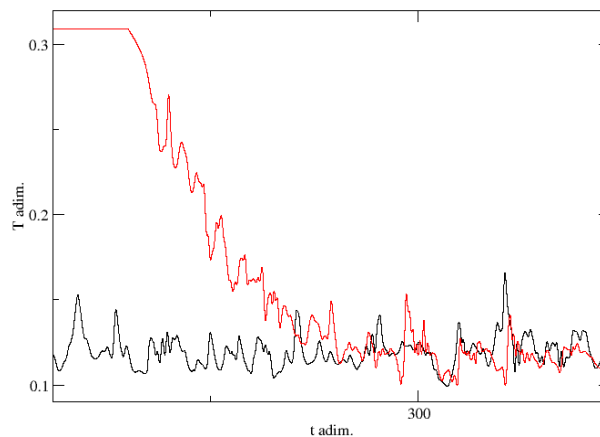


Figure 5: Temporal temperature evolution with radiation since the beginning (black) and with radiation from the convection steady state (red) at a same point (0.5, 0.5, 0.875).

Figure 5 shows that if we apply radiation on the convection steady state, the new configuration tends towards the same asymptotic situation that we would have if we start radiation calculations from the beginning. With this particularity, it may be easier to reach

a permanent state. This might be very interesting in case of a low coupling frequency which demands very high calculation resources.

2.2.4 Conclusion of the 3D natural convection / radiation coupling project

During this project, we have developed a strategy to simulate coupled 3D natural convection and radiation in high Rayleigh number cavities for possible application to thermal efficiency of buildings. Flow equations were solved using a pseudo-spectral method associated with a multi-bloc parallel code. Radiative transfer, including surface and volume contributions, was calculated using a Monte Carlo method (MCM) and a line by line description of molecular spectroscopic properties.

The main difficulty encountered during the last period of this project was related to MCM convergence at very low temperature differences. This problem was solved using a superposition method and the required computational times became reasonable.

The first coupled calculations were carried out for a Rayleigh number $Ra = 3 \cdot 10^7$. They already show very interesting results such as the tendency of radiation to destabilize the boundary layers and to yield unsteady and chaotic behaviours for configurations for which pure natural convection yields steady flows (see [24]).

For future calculations we need to increase the Ra number to reach the value we have in our experimental cavity i.e. $Ra = 10^9$ (see [26]). This implies an important increase of mesh cell numbers and Monte Carlo events, and consequently, a high increase of calculation times.

2.3 Conclusion

Works realised in the Natural convection / Radiation project allowed us to have a 3D application release ready for large or very large scale numerical simulations and obtain, through 2D case studies, relevant information such as coupling frequency, etc. The first 3D numerical simulations confirmed important effect of radiative heat transfer on natural convection flow observed previously on 2D cases.

The 3D release makes feasible large-scale 3D numerical simulations of the coupling of natural convection with radiative heat transfer in a mixture of air, water vapour and carbon dioxide and will be able to provide reference numerical solutions. The reference results are necessary not only for pure numerical comparison exercises but also for determining the minimal radiative transfer model in the building context.

Future works consist of setting up less expensive 3D approaches of radiative transfer in the 3D application release and determining the minimal radiative transfer model in the building context on the one hand and performing numerical simulations for LET experiments on the other hand.

3. FOCUS project

<i>Title</i>	Full coupling between radiatiOn and Combustion for Unsteady Simulation (FOCUS).
<i>Scientific leader</i>	Olivier Gicquel, EM2C (Laboratoire d'Energetique Moléculaire et Mascroscopique, Combustion), Chatenay Malabry, France.
<i>Partner Laboratories</i>	CERFACS/IMFT (Institut de Mécanique des Fluides de Toulouse), Toulouse, France.

In this section we are going to report on changing the coupling technology of the coupled application and on the last scientific results obtained in the FOCUS project (DECI project).

3.1 Using PALM technology

3.1.1 Overview

PALM [11] is a coupling technology developed by the *Global Change and Climate Modelling* team at the CERFACS laboratory. This technology was originally designed for an oceanographic project called MERCATOR to provide a flexible and efficient way to build the Data Assimilation system in operational context. Today PALM software is widely use in different scientific domains to couple complex codes as for instance: environment coupling projects, fluid/structure coupling, fluid/radiative/structure coupling, neutronics coupling. The aims of this task are first to measure the impact of the technology switching, and to study how to deploy the application in HPC context as DEISA.

Briefly a PALM application consists of modules/components called *PALM units* which can be assembled with the help of a GUI called PrePALM. The *PALM units* are associated with Fortran subroutines, C or C++ functions. Each *PALM unit* is associated with an *identity card* which describes how to build the *unit* and the input/output (consumed/produced) data type. The *units* can be gathered into one or several executables named, called with the PALM terminology *branches*. PALM can manage two levels of parallelism: the internal parallelism of the *branch/unit* (shared or memory distributed parallelism) and the parallelism offered by executing several concurrent *branches*. PALM provides advanced mechanisms allowing to redistribute data between several parallel *branches*. Useful tools complete this very user-friendly software: algebraic operations between objects, debugging tools and performances analyser.

3.1.2 Implementing PALM technology

As seen in previous paragraph, the PALM concept is to assemble complex and parallel applications in a modular way and to offer to users extensible applications.

The CORBA technology which encapsulates and couples the two codes `AVBP` and `DOMASIUM` has been changed with PALM one. This operation has been done by just rewriting the two files which encapsulated the two codes. These two files have been renamed in `rht_palm.f90` and `avbp_palm.f90`. In each file, all CORBA invocations have been converted with basic communications PALM calls (`PALM_get/PALM_put`) and the links with the legacy codes have been reconnected. Then the *identity cards* associated with the 2 previous files has been directly obtained from the CORBA IDL by converting

the description of input/output data. The similarity of the two description files is obvious, see Figure 6-a. The next operation consists to change all MPI_COMM_WORLD communicators with the one provided by PALM (this operation should be simple if MPI calls were built on a local application communicator, i.e. not directly on MPI_COMM_WORLD) and to suppress the MPI initialisation and termination (MPI_INIT and MPI_FINALIZE). To end the PALM implementation, two branches and two units were created in the PALM GUI PrePALM, associated with the legacy codes and then interconnected to couple them (see Figure 6-b).

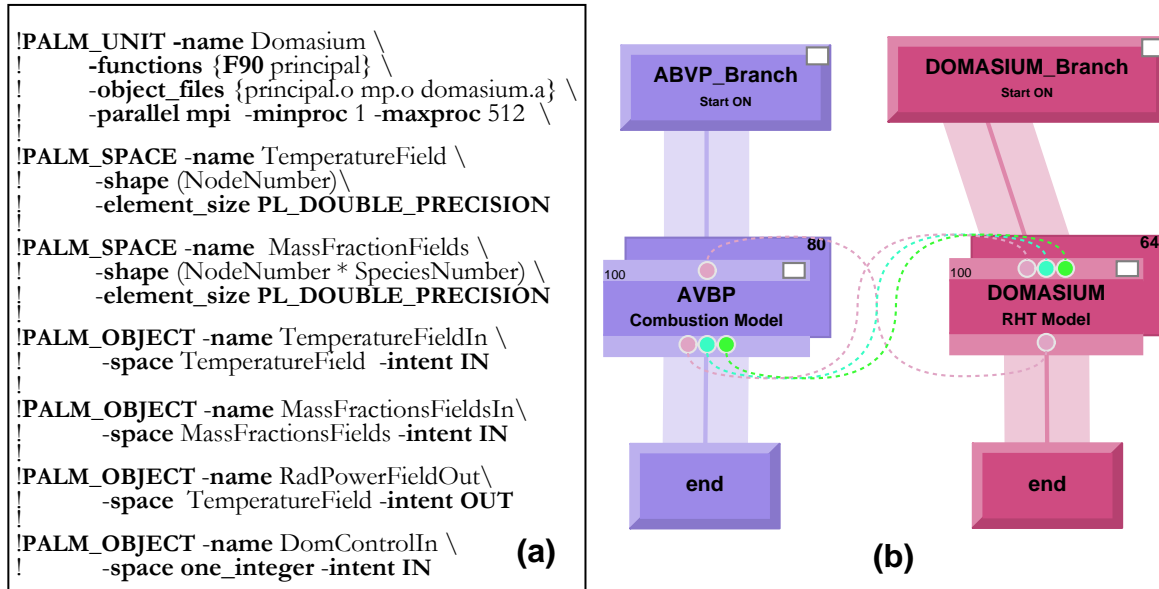


Figure 6: (a) Extract of the DOMASIUM *identity card* and (b) coupling module with PrePALM tool.

Coupling with CORBA technology provides a high level code organization which greatly simplifies this technology substitution. According to the best suited coupling technologies available in DEISA infrastructure, we are able to switch quickly to new coupling technologies.

3.1.3 Deployment on the DEISA infrastructure

The PALM software depends on the MPI library used; it requires the MPI-1 version with MPI-2 extensions as the *dynamic process management*. PALM was well suited with the communication library LAM-MPI which is today obsolete and replaced by the OpenMPI implementation.

Because some of the DEISA platforms do not support the MPI-2 subset (*dynamics process management*) it is not trivial to launch a PALM application in this context. It is always possible to run the coupled application by using an MPI implementation based on a non native library, but it will decrease drastically the performances. Another approach is to merge the 2 codes in a unique one, avoiding in this way the use of the *dynamics process* subset, but this will restrict strongly the coupling possibilities.

3.1.4 Conclusion

The PALM software has been designed in an intelligent way and offers a user-friendly way to couple applications. Changing the coupling technology was rather simple and confirmed our choices in the coupling organization. These good characteristics of PALM have insured a real success of this software to couple applications and it will be very

interesting if this tool, like other coupling tools, can be deployed conveniently and efficiently on HPC platforms.

3.2 *DECI simulations — numerical results*

First results on the gas turbine simulation which are presented in the next, lead to improve the radiative code by taking account of wall radiative properties. In a second time, these new features were validated on the well-known configuration the 3D diedra.

3.2.1 *Gas turbine simulation*

The gas turbine simulation was realised for two different meshes. This configuration was used to validate all the computational tools developed in this project. Test with more than 400 processors was made and the two coupled codes didn't degrade the performance. Analyses from the results shows that the boundary condition set in the radiation code have a hard influence in the temperature field. Firsts simulations were carried out assuming blackbody condition for the walls ($\varepsilon = 1$). Like we can see in the Figure 7 with this configuration, the mean temperature field was almost the same with and without radiation, which is physically incorrect.

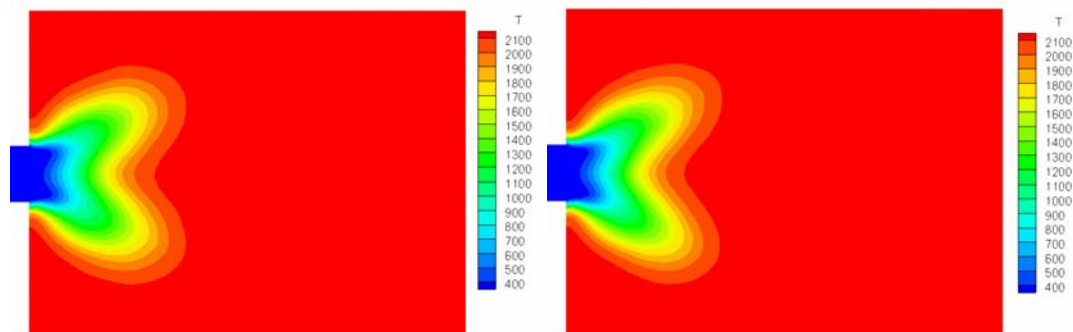


Figure 7: Mean resolved temperature field in the central plane of the burner ($z=0$), without (left) and with (right) radiation.

A new boundaries condition was developed. In the new version of the radiation code, an emissivity ε is specified for each different wall. It is assumed to be constant for the ceramic walls ($\varepsilon = 0.91$) while the real curve of the material emissivity in function of the wavelength is retained for the quartz walls (semitransparent at short wavelengths becoming opaque at longer wavelengths) the others walls and obstacles were assumed to be cold blackbodies, $\varepsilon = 1$: all rays reaching the walls are absorbed (no reflection and no transmission). The quality of the results improved with these new assumptions, the maximums values in the power radiation field absorbed by the fluid have been reduced and lower temperatures for the coupled case were achieved.

One last simulation was done for the diedra case. The choice of this configuration comes from the possibility to compare the 3D simulation with the 2D simulation done before (see previous deliverable [13], [14] and see recent publications [17], [18], [19] and [21]) also to compare with a large number of experimental results already available at EM2C laboratory.

3.2.2 *Diedra simulation*

Simulation description

The three-dimensional computational domain (see Figure 8) starts 10 cm upstream of the flame holder and continues up to 30 cm downstream. It contains about 2.6 millions cells (tetrahedrons), and the maximum grid size downstream of the flame holder is $\Delta = 1.6$ mm. The same mesh is used in AVBP and DOMASIUM. In the following simulations, the AVBP time step is about $\Delta t_{LES} \sim 0.2 \mu s$.

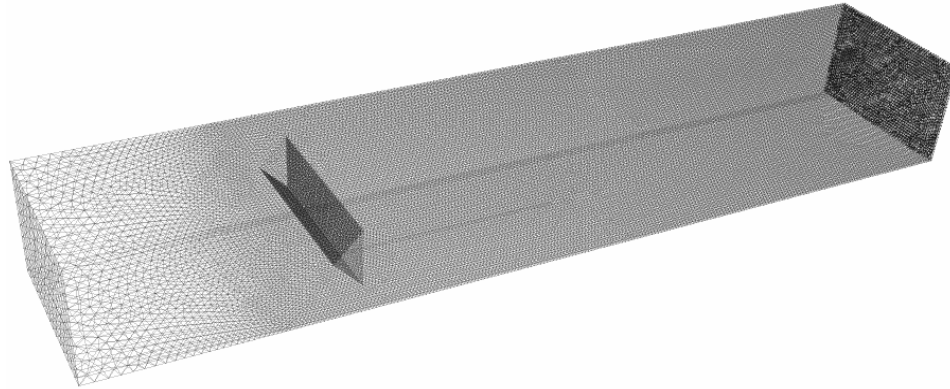


Figure 8: 3D Mesh of the flame holder with 2.6 millions of tetrahedrons.

A heat flux condition is imposed in the combustion code, estimating different thermal resistance for each wall and for the aluminium triangular-shaped flame holder. In the radiation code, an emissivity ε is specified for these walls. It is assumed to be constant for the ceramic walls ($\varepsilon = 0.91$) while the real curve of the material emissivity in function of the wavelength is retained for the quartz walls (semitransparent at short wavelengths becoming opaque at longer wavelengths) the others walls and obstacles were assumed to be cold blackbodies, $\varepsilon = 1$: all rays reaching the walls are absorbed (no reflection and no transmission).

Preliminary studies have shown that exchange of information each 100 interactions AVBP is a good compromise between results precision and computing time. A correct load balancing is then achieved by devoting 40% of the processors to the LES code AVBP and 60% to the radiative heat transfer code DOMASIUM. Typical runs have been conducted using 160 processors (64 for AVBP, 96 DOMASIUM) and well succeed tests cases were carried out using more than 400 processors in total.

Results and Discussion

Calculations without radiative heat transfer, using only the AVBP code, have been carried out to provide a reference case referenced NR in the following. To perform relevant comparisons of the flow fields without and with radiation at the same instant, both computations start from a time $t_0 = 0,415$ s of a previous computation that does not take into account radiative heat transfer.

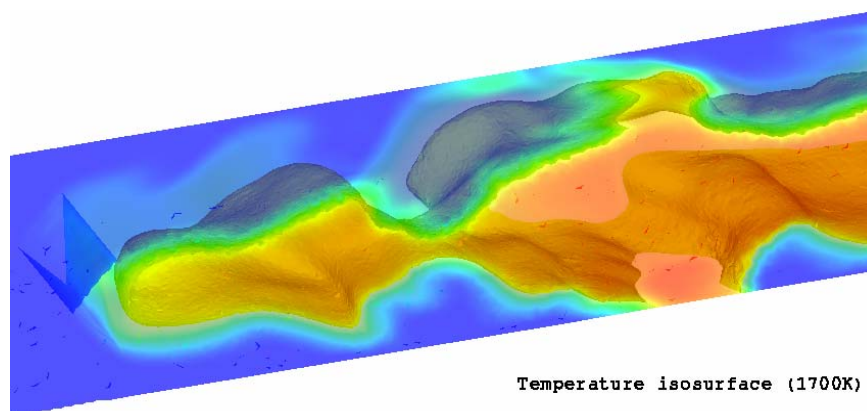


Figure 9: Isosurface of the instantaneous resolved temperature (1700K) at time $t = 0.55$ s

The Figure 9 displays a typical view of a resolved temperature isosurface and evidences the three-dimensional behaviour of the flow field. Figures below compare the mean resolved temperature (Figure 10) and CO_2 mass fraction fields (Figure 11) in the centre plane ($z = 0$) without and with radiative heat transfer, respectively. First, as expected, the maximum mean temperature is decreased by about 100 K, because of the increase of energy transfers from hot to cold zones and to walls due to radiation. These temperature differences directly impact the reaction products. For example the mean CO_2 mass fraction is slightly decreased when radiation is included. These observations are confirmed by Figure 12, where transverse profiles of the same physical variables 5 cm downstream of the flame holder are presented. A more significant impact of radiative heat transfer may be anticipated when using a more detailed chemical mechanism including pollutants such as carbon monoxide (CO) or nitric oxides (NO_x), known as very sensitive to local temperature.

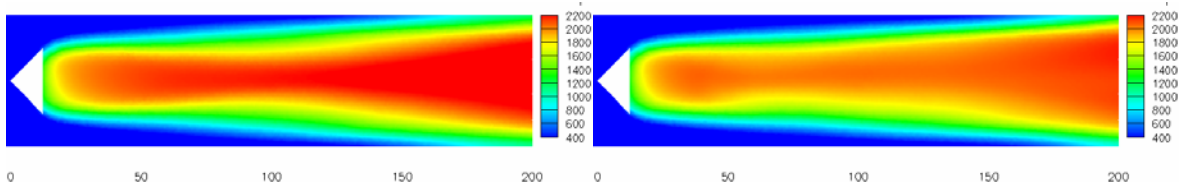


Figure 10: Mean resolved temperature field in the central plane of the burner ($z=0$), without (left) and with (right) radiation.

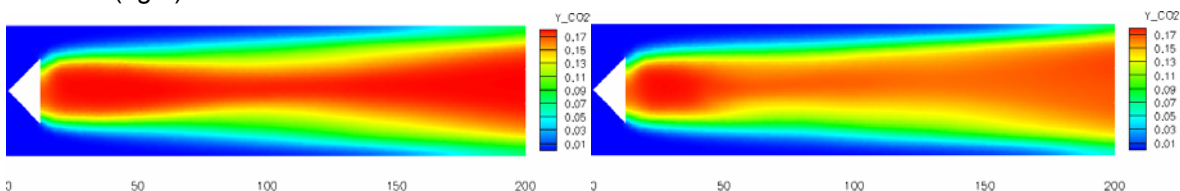


Figure 11: Mean resolved CO_2 mass fraction field in the central plane of the burner ($z=0$), without (left) and with (right) radiation.

Figure 13 compares instantaneous field of the resolved temperature at the same physical time $t = 0.55$ s. As expected, the maximal temperature decreases when radiative heat transfer is included, especially in the recirculation zone just downstream of the flame holder, which plays a key role in the flame stabilization mechanism. Indeed, modifications of the temperature field in this region may induce deep changes in the flame behaviour and its interaction with turbulence motions.

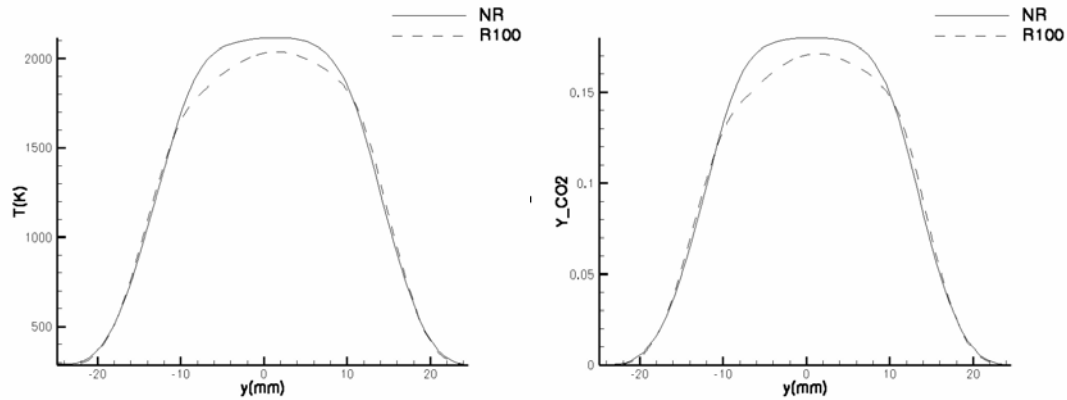


Figure 12: Transverse profiles of the mean filtered temperature (top) and CO_2 mass fractions (bottom) in the central plane of the burner ($z=0$), $x=0.05$ m downstream of the flame-holder without (NR) and with (R100) radiative heat transfer.

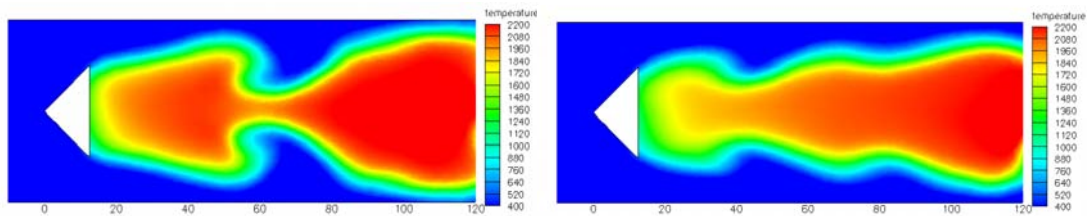


Figure 13: Instantaneous resolved temperature field in the central plane of the burner ($z = 0$) without (left) and with (right) radiative heat transfer at the physical time $t = 0.55$ s.

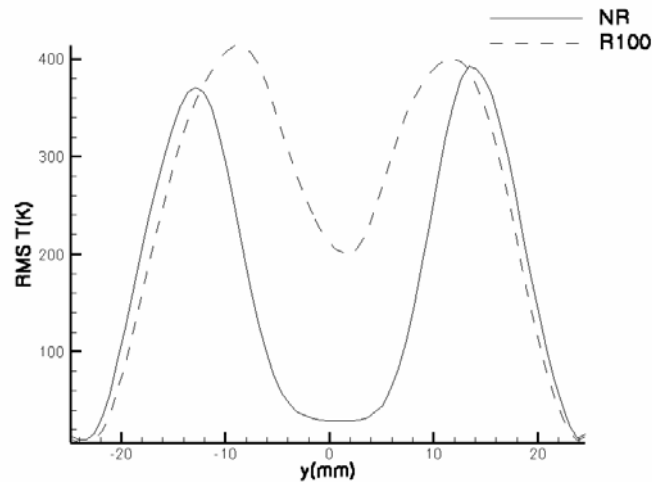


Figure 14: Profiles of the filtered temperature RMS in the central plane of the burner, ($z=0$), $x = 0.05$ m downstream of the flame holder without (NR) and with (R100) radiative heat transfer.

The filtered temperature RMS (root mean square), that measures the variation around the mean temperature, more quantitatively evidences the modification of the flame dynamics when radiative heat transfer is taken into account, as shown in Figure 14. This figure compares the filtered temperature RMS profiles in the central plane of the burner 5 cm downstream of the obstacle without and with radiation. RMS values are clearly larger when radiative heat transfer is taken in account, denoting stronger flame

movements. The maximum value is increased by about 50 K while values higher by about 200 K are observed on the chamber axis ($y = 0$). These findings confirm that the strong influence of radiative heat transfer in spite of its limited contribution to energy transfer (less than 2 % of the overall heat release).

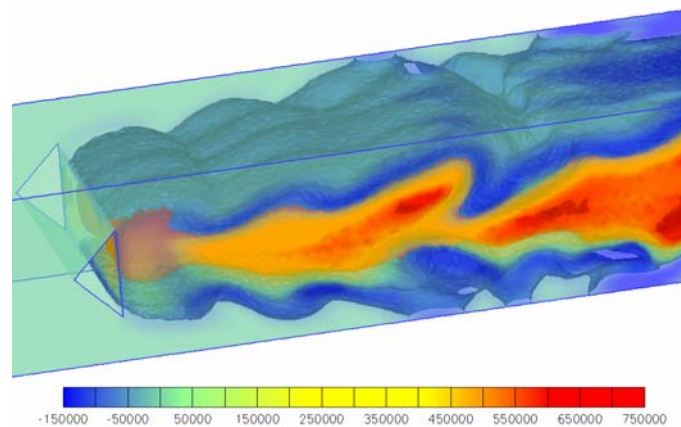


Figure 15: Instantaneous field of the radiative power (in KW.m-3). Positive (respectively negative) radiative powers are lost (absorbed) by gases.

Figure 15 displays an instantaneous field of the radiative power. A large positive central zone corresponds to the radiation power emitted by the burnt hot gases. A small absorption zone is visible upstream of the flame front.

All these recent results have been submitted to *Combustion and Flame* and are going to be detailed in a PhD thesis [22] prepared at EM2C laboratory.

3.3 Conclusion and future work

Radiative heat transfer plays an important role in the turbulent combustion, but is often neglected in simulations because of its complexity and the related numerical cost. An original approach has been used to perform numerical simulation of unsteady 3D turbulent combustion including radiation. Two independent Fortran codes, one for large eddy simulation of turbulent combustion, the other to estimate radiative heat transfer, exchange data through a specialized framework CORBA preserving the individual code performances. This coupling technique is simple to implement, portable, flexible and versatile. In the case of the DECI project two different cases of these huge calculations have been performed proving the importance and viability of this kind of coupled simulation.

Results from the three-dimensional simulation of a turbulent premixed propane / air flame stabilized downstream of a triangular shape obstacle show that taking into account radiative heat transfer in reactive large eddy simulations greatly modifies the flame dynamics, the temperature and fraction species fields, in spite of a limited impact on total heat release transfer. These results evidence the importance of radiation heat transfer in turbulent combustion and show the relevance of the proposed procedure.

The three-dimensional simulation results compared with the two-dimensional case give us the opportunity to validate the impact of radiation on the turbulent phenomena in the combustion chamber and to show the importance of the boundary conditions for the radiation code.

Future studies should be devoted to improve the wall boundary description, taking into account the radiative flux, the interaction of the thickened flame model with the radiation and the possibility to use different meshes for each code.

4. The KOP3D project

<i>Title</i>	Kopplung 3D (KOP3D).
<i>Scientific leader</i>	Claus-Dieter Munz, IAG (Institut für Aerodynamik und Gasdynamik), Stuttgart University, Germany.
<i>Partner Laboratories</i>	Numerische Simulation und Auslegung eines instationär gepulsten magnetoplasmadynamischen Triebwerks für eine Mondsonde – Project of the "Landesstiftung Baden-Württemberg".

4.1 *Current Scientific Usage and Improvements*

KOP3D is used to calculate aeroacoustic flows with noise generation and noise propagation together in a single simulation and thereby respecting interactions between those two flow phenomena. For a better simulation of noise generation the full Navier-Stokes equations have been implemented in the solvers of KOP3D since the last deliverable. So it is now possible to simulate viscous flows and their acoustic behaviour with KOP3D. Some first simulations of the von Karman vortex street have been done using this new feature. This incorporation of the full Navier-Stokes equations puts the KOP3D on a new level of realism but increases also the demand for computational power of the application. The goal is today to compute large 3D aeroacoustic problems with an until now unknown high fidelity in realism.

4.2 *Reduction of Coupling Loads*

The needed calculation power to fill the values at the spatial resolution (Gaussian integration points) along the interfaces has proven to be large enough to be a burden to the simulation. This is especially true for domains with structured meshes. A frequently used configuration of domains is one, where a domain with an unstructured mesh is embedded into a set of domains with structured meshes. As the solver for domains with structured meshes was only able to handle rectangular domains, it was necessary to set up a ring of domains around the central domain. This resulted in large interfaces between the domains in this ring due to the huge area which is needed to simulate the sound wave propagation. In order to avoid these unnecessary interfaces the structured solver was enhanced.

The solver for domains with structured meshes can now handle "holes" within the domain. This way, parts of the domain can be excluded from calculation and can instead be used as coupling ghost cells. By this enhancement it is now possible to avoid the artificial large interfaces in a surrounding ring of domains and use a single domain instead. The number of Gaussian integration points (Gaussian integration points) needed to be calculated for the coupling is so drastically reduced.

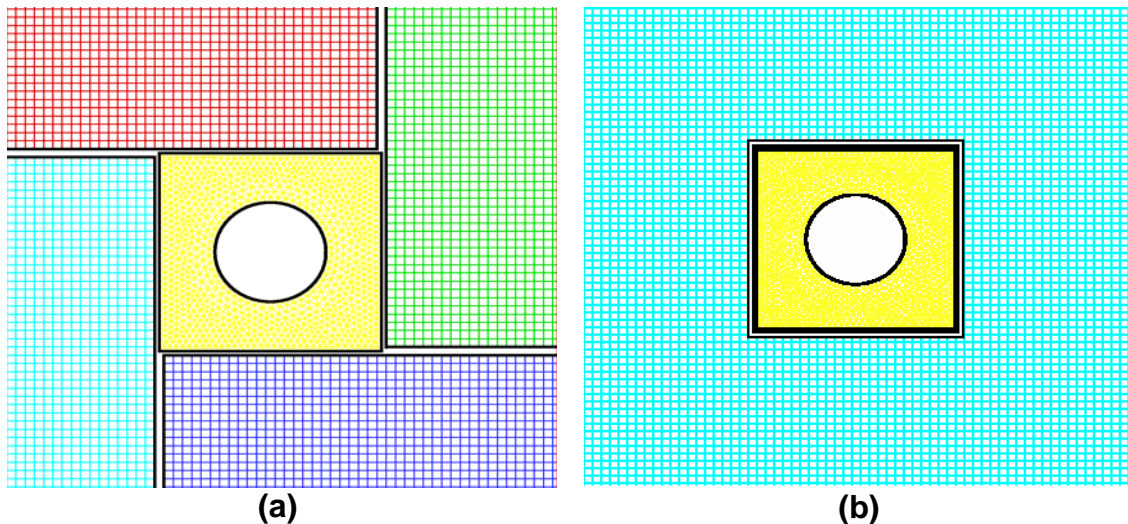


Figure 16: (a) Unstructured Domain surrounded by ring of rectangular domains; 22 % time spent in the coupling subroutines. (b) Unstructured Domain embedded in structured domain with a hole; 7 % time spent in the coupling subroutines.

As an example for this reduction, the simulation of the scattering of a time harmonic plane sinusoidal acoustic pressure fluctuation at a perfectly reflecting cylinder is shown in Figure 16-a. The domain configuration in this example is exactly as described above: there is a domain with an unstructured mesh around the cylinder in the centre, which is surrounded by an area of structured meshes. In the old configuration four rectangular domains were necessary to build a ring around the central domain (see Figure 16-a). With the enhanced solver for structured meshes only one domain is necessary into which the central unstructured mesh with the cylinder can be embedded (see Figure 16-b).

Each configuration is run with two processes, one process calculated the central domain and the other process calculated the four structured domains in the old configuration or the single outer domain with the hole in the new configuration. On a local x86 architecture this reduces the time spent in computing the coupling information from around 22 % of the total time spent in the structured solver to around 7%. The total time spent in the structured solver is reduced by nearly 18%. On the SX-8 a similar reduction of the execution time for the structured solver is gained (about 17%).

This improvement of the structured domain solver increases the scalability and usefulness of the coupling scheme by eliminating unnecessary coupling computations. The speed up gained by the adapted sub domains is thereby amplified by the reduction of the needed coupling overhead. This makes KOP3D an even more valuable tool for aeroacoustic simulations.

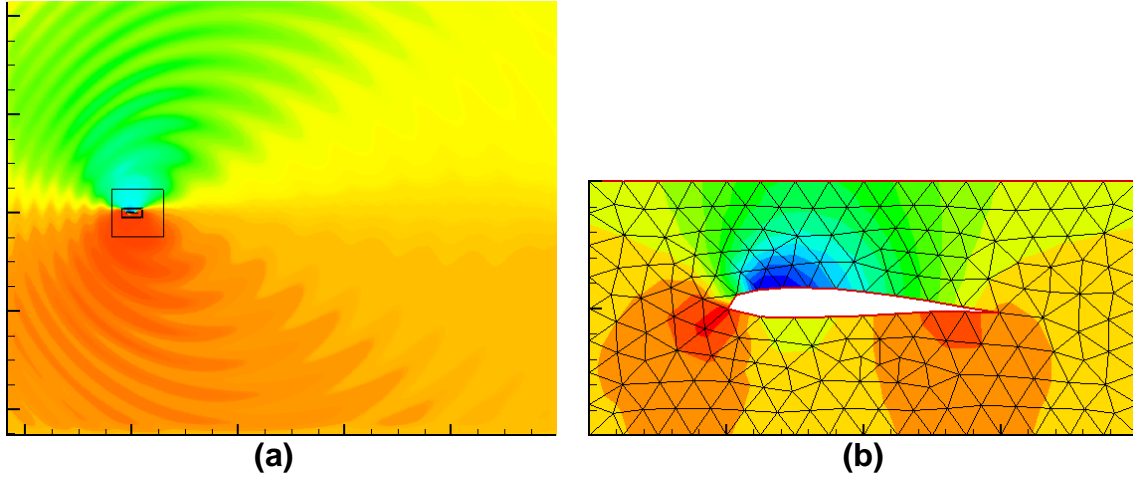
4.3 *Heterogeneous Parallelism*

The work on interoperability of the program with the PACX-MPI library has been completed. The PACX-MPI library has been installed at IDRIS and tested successfully between the two sites HLRS and IDRIS. Recently we have started porting KOP3D to the AIX architecture available at IDRIS. This work was not completed during the reporting period.

However heterogeneous parallel simulations were performed between the NEC SX-8 and an IA64 Linux cluster which actually serves as front-end server for the vector machine.

Figure 17: Domain configuration in (a) with two structured domains and one unstructured domain. Close up of the unstructured mesh with the profile is represented in (b).

The used test case is a benchmark problem by Scott [29] in the field of computational



aeroacoustics. In the KOP3D framework the problem is split up in a mixture of structured and unstructured domains. The structured domains are well suited for vectorization and thereby exploit the features of the NEC SX-8 processors. Whereas the unstructured solver in KOP3D is based on element wise calculations which is taking disadvantages from running on the vector architecture. For validation of the PACX-MPI library usage the aeroacoustic gust response of a single Joukowski profile is simulated (see Figure 17). For this simulation an unstructured domain at the centre around the profile is used, where the nonlinear Euler equations are solved. This domain with the unstructured mesh around the profile is embedded into a domain with a structured mesh and a hole for the central unstructured domain. On this domain still the nonlinear Euler equations are solved. Finally there is a coarse structured mesh around the other two domains, where linearized Euler Equations are solved. The unstructured domain is calculated on the IA64 Cluster and the two structured domains are run on the NEC SX-8. As can be seen, we take advantage of the newly introduced feature for holes in structured meshes. This simulation and its runtime results are presented in [28].

	Heterogeneous platform (IA64 and SX-8)	IA64 platform	SX-8 platform
Structured domain	7	196	7
Unstructured domain	326	324	840
Total	333	520	847

Table 1: Runtimes of the airfoil gust simulation on scalar IA64 platform, a NEC SX-8 platform and on an IA64 / NEC SX-8 heterogeneous platform (coupled with PACX MPI Library)

As shown in Table 1, the runtime for the whole program can be reduced by nearly 36 % in the distributed run when compared to the simulation on the scalar cluster alone. This advantage is of course dependent on the chosen testcase and the optimization of the corresponding routines to the underlying architecture. However, as this typical testcase of the application demonstrated, a real reduction of time is possible by this approach, that is not achievable by other means.

In order to do the mapping of the numerical requirements in the different domains onto the different architectures, a feature to determine on which machine the process within

the PACX-MPI world is running was implemented into KOP3D. By this feature each MPI process is aware of the machine it is running on and it is possible to pick a set of domains for it accordingly. This feature is accessible in a convenient way by a command line option to the program.

Besides the greater availability of the tool by porting it to different architectures, this enabling of heterogeneous runs enhances the options of how big problems may be distributed without losing performance or even gaining advantages by exploiting the different architectures in an optimal way.

4.4 Improvements on Load Balancing

The load balancing mechanism has been improved. In the context of the parallel KOP3D the problem arises of how a given number of processors is mapped onto the physically given domain layout. Previously this was done using a very simple algorithm, called “all for all” distribution, where each processor calculated a small fraction of each domain. This naïve approach for processor distribution results in a nearly perfect load balance, as the needed calculation time is nearly constant across a single domain. However this results in a lot of fragments, that need to communicate with each other over MPI. The fast increasing number of fragments which is number of processors times number of domains, reduces the scalability. For a greater number of processors it is therefore necessary to use a different algorithm for the processor distribution.

So in a newly implemented algorithm it is now possible to distribute the processors on the given physical setup of domains in a way that domains are not split across more processors than necessary. This new distribution of course reduces the quality of the balance but the load balance is already quite good, also it may be further improved. The needed communication is thereby reduced in comparison to the previously used distribution scheme, where each processor would calculate only a small part of each domain.

Instead of the otherwise needed MPI communication within each sub-domain due to lots of sub-domain fragments, the fitting of the processes to the sub-domains leaves the communication mainly to the coupling interfaces. At these interfaces between neighbored sub-domains expensive communication overhead like interpolation and restriction has to be done additionally to the data exchange anyway. So the needed MPI communication is not the driving factor here anymore.

For the analysis of the new load balancing scheme the simulation of a co-rotating vortex pair is used. This example contains nine rectangular domains with structured meshes. We don't take advantage of the newly implemented feature of holes in the structured domains here, which wouldn't change much in this context.

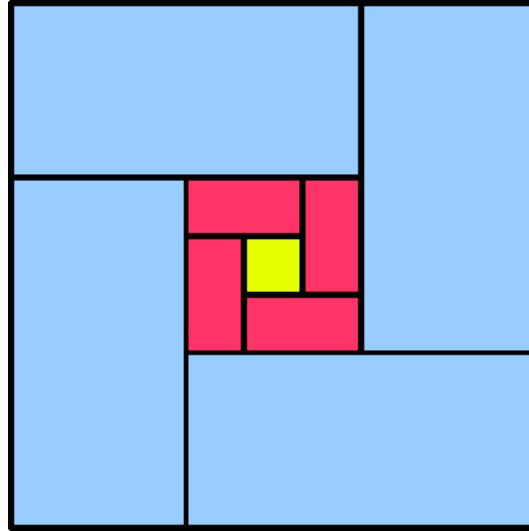


Figure 18: Set configuration of the nine domains in the co-rotating vortex pair example.

The co-rotating vortex pair itself is simulated in a mesh of high resolution at the centre using nonlinear Euler equations. Adjacent to the central domain is a ring of domains with a coarser mesh on which still the nonlinear Euler equations are solved. In the outermost ring of domains simulating the far-field, only a coarse resolution is used to calculate the flow with linearized Euler equations. This configuration of domains is shown in Figure 18.

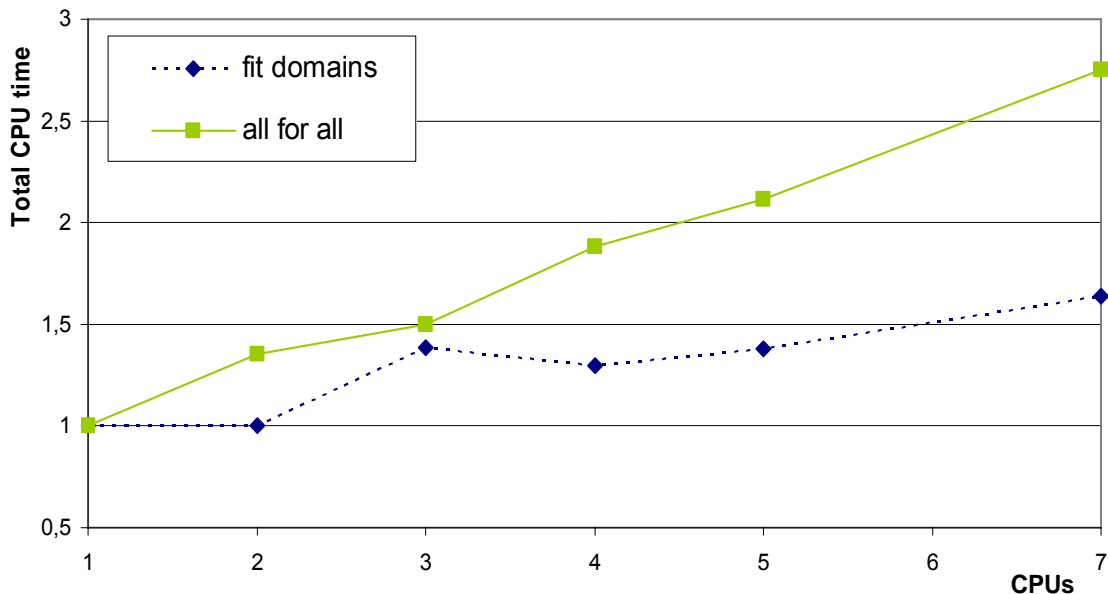


Figure 19: Comparison of the two distribution modes. In green each process calculates a small part of each domain. In blue the processes are fitted to the domains.

As shown in Figure 19 the overhead can get dominating and the old “all for all” distribution has a quite bad scaling. This overhead is not only due to the communication but also to the reduced problem sizes which decrease the average vector length. These small problems have an especially high impact on the vector architecture. By fitting the processes to the domain configuration the scaling can be greatly enhanced due to the reduced communication and increased problem sizes. The analysis was done on the NEC SX-8 with a constant problem size.

The newly introduced distribution scheme requires the specification of the load generated by each domain. Ideally this would be determined during runtime, as for nonlinear problems this may change unpredictable over time, but a dynamic load balancing is still quite expensive, as it requires providing of the whole coupling information each time a rebalancing is done. So currently only a static distribution, given at start-up time is supported.

Implementing load balancing was a vitally important feature for KOP3D to run efficiently in a parallel environment. It greatly enhances the potential of the already flexible concept of domain coupling used in the project to solve huge problems.

4.5 Conclusions

Through the work in the DEISA project the possibilities of KOP3D have been greatly enhanced. The parallel implementation is a necessity for calculations of big problem sizes. Enabling parallel coupling between already parallelized domains opens the access to totally new problem classes.

For example the solving of the complete Navier-Stokes equations has been implemented with the prospect of the parallelized KOP3D. Thereby it is possible to simulate the overall physical effects of aeroacoustics from the noise generation, including viscous effects, to the propagation of the sound waves. So the problem sizes are already huge in 2D simulations, when including the complete Navier-Stokes equations. They become really complex and demanding in terms of needed calculation power in 3D simulations.

The different scales of the physical phenomena looked at in the field of aeroacoustics make a decomposition necessary, without mechanisms like those in KOP3D it won't be possible to simulate the generation; of the noise at an object like an airfoil that may be of the size in meters and the propagation of the generated sound waves over large distances to an observer, that may be kilometres away from the point of noise generation in the same simulation. The calculation in a single simulation context is necessary to reproduce the physical effects of the interactions between the different flow phenomena.

Simulations of the 2D vortex street were already performed in the parallel context and provide a promising outlook. The increased diversity of the physical domains may prove to be even better suited for the heterogeneous super computing environment.

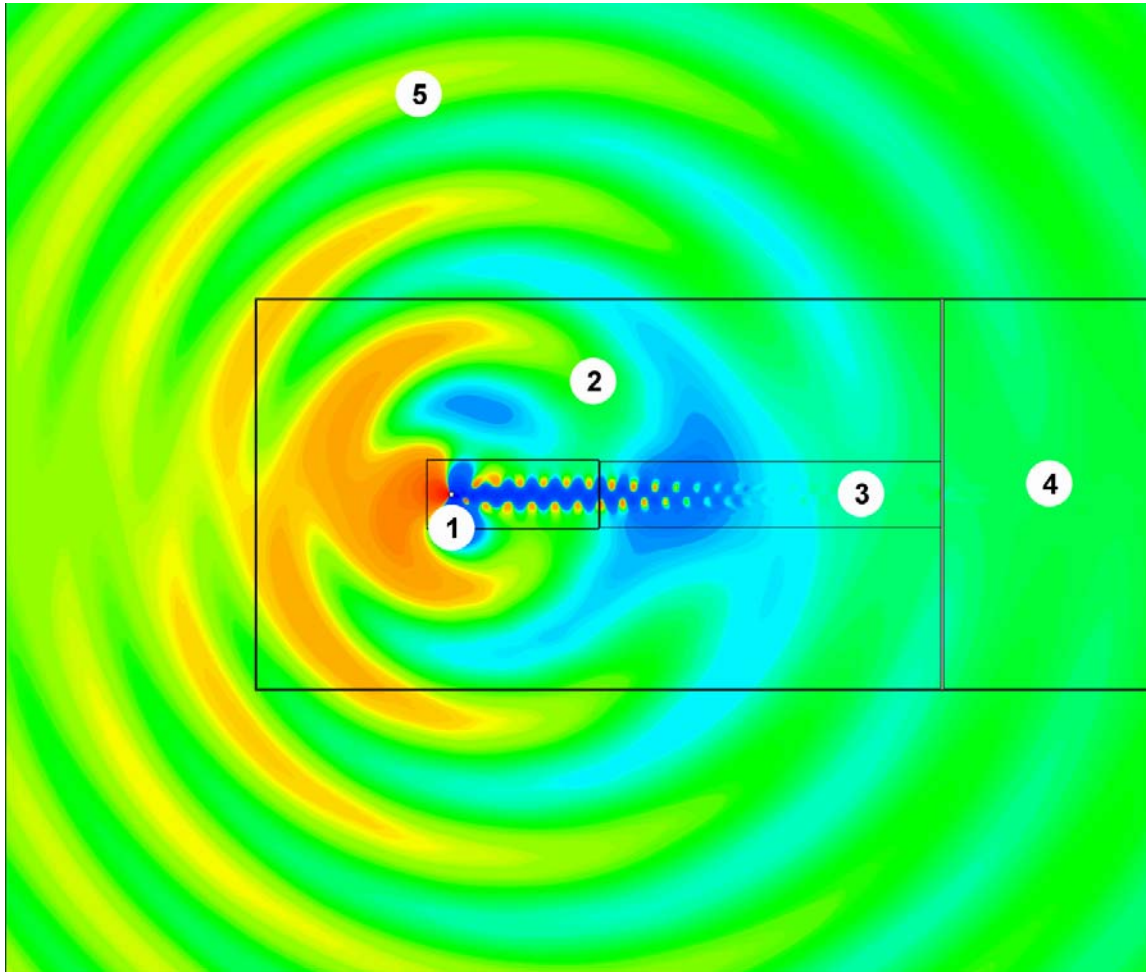


Figure 20: Visualization of the pressure field generated by a von Karman vortex street decomposed into (1) unstructured Navier-Stokes, (2) structured nonlinear Euler, (3) structured Navier-Stokes, (4) structured nonlinear Euler and (5) structured linearized Euler.

The decomposed set up of such a 2D von Karman simulation is presented in Figure 20. Shown is the resulting pressure field of the simulation with domains of different physical properties. In domains (1) and (3) the full Navier-Stokes equations are solved. In domains (2) and (4) the nonlinear Euler equations are solved. On domain (5) finally, which serves as the far field, linearized Euler equations are solved. Domain (1) is the only unstructured part in this configuration, all the other domains have structured meshes.

So with the work done in DEISA and the recently implemented Navier-Stokes equations it is now possible to simulate aeroacoustic problems with a level of detail and realism never reached before. However there are still some small parts in KOP3D to improve the parallelism. In proposal is a 3D simulation of the noise generated by the Von Karman vortex street.

5. New projects

In this last section we present the new projects selected for the next 12 months activity.

5.1 *Fluid / structure coupling (BACI)*

<i>Title</i>	BACI project.
<i>Scientific leader</i>	Prof. Wall, Lehrstuhl für Numerische Mathematik (LNM), Munich, Gemany
<i>Links with other scientific projects</i>	CCARAT (Computer Aided Research Analysis Tool) project, University of Stuttgart.

BACI is a fluid / structure coupling project, which is developed by Prof. Wall at the LNM (Lehrstuhl für Numerische Mathematik) in Munich. This project is a branch of development from CCARAT and is already used on parallel architectures.

5.1.1 *Scientific project*

The aims of this project are to study the transient interaction of incompressible viscous flows and nonlinear flexible structures (like for instance bridges oscillation under high wind pressure and several medical cases). BACI is a research finite element code designed to solve a large range of problems in Computational Fluid and Solid mechanics:

- multifield, multiscale and multidiscretisation schemes,
- shape and topology optimization problems
- material modelling and element technology aspects.

5.1.2 *Objectives in this Joint Research Activity*

The different physics involved in this simulations show quite different numerical requirements and coupling interaction is well restricted. It may be possible to take advantage of the heterogeneous computing architectures for the different physical simulations. It is planned to use the BLIS (Block Linear Iterative Solver) Library, developed at HLRS in the fluid solving part of BACI and thereby gaining high performance on the NEC-SX8. The field of fluid / structure coupling has high demands in terms of calculation power, as the purposed 3D simulations need high resolution in time and space for the interaction of the different physics involved.

5.2 *Molecular Dynamics / Visualisation project*

<i>Title</i>	Driving Molecular Dynamics simulations with a High Performance Visualisation tool (MDDriver).
<i>Scientific leader</i>	Marc Baaden, Laboratoire de Biochimie Théorique at IBPC research institute (Institut de Biologie Physico-Chimique), Paris, France.
<i>Partner Laboratories</i>	Prof. Mark SP Sansom, Structural Bioinformatics & Computational Biochemistry at the University of Oxford, United Kingdom

5.2.1 *Scientific project*

Recent findings in the nano- and life sciences have shown an unsuspected general importance of the mechanical properties of (macro)molecules and their assemblies, as

for instance in enzymatic activity or membrane fusion. Some understanding of these properties can be gained by large-scale computer simulations. Our recent 340,000 atom simulation of the SNARE complex involved in membrane fusion is one such example, the investigation of enzymatic active sites is led under tension another. Interactive Molecular Dynamics (IMD) is one particular method where a simulation is coupled with an interactive visualisation in order to drive the system towards the relevant degrees of freedom. In order to be able to carry out IMD simulations on our systems we need to couple our current simulation code with an interactive visualisation tool. This will enable us to apply stress to the system and visualize the strain propagation. The interactive coupling is important as different applied forces need to be tested in order to locate particularly weak or rigid spots. On-the-fly visualisation helps identify them. Doing this systematically and without interactive control is either not feasible or results in an important waste of computing time on "un-productive" cases.

5.2.2 Objectives in this Joint Research Activity

The aim of this activity is to provide a powerful and flexible coupled application connecting large-scale molecular dynamics simulations with advanced and interactive CPU intensive visualization.

Today the well known coupled application NAMD/VMD is a reference in massively parallel molecular dynamics software enabling novel simulation methods like "Interactive Molecular Dynamics" (IMD). The software is largely used by the biomolecular simulation community. Nevertheless the models and simulation methods provided by NAMD cannot easily be extended and lack some functionality like e.g. implicit solvent models and efficient minimization algorithms. The graphics part VMD is limited by the fact that its visual representations cannot easily be extended and large simulations can pose a performance problem as VMD can only run on a single computing node. In this JRA6 activity we propose to progressively change these two modules. First the molecular dynamics module will be replaced with the well known European molecular dynamics code called GROMACS, and second, the graphical part will be replaced with a more scalable code based on the VTK framework. VTK can make use of available CPU power to deliver complex visualisation tasks and can easily be extended with new representations. This activity will permit to have a new coupling experience with molecular dynamics codes and to transmit our knowledge in coupling technology to the research teams involved.

5.3 Quantum Mechanics / Molecular Mechanics project

<i>Title</i>	Quantum Mechanics / Molecular Mechanics coupling
<i>Scientific leader</i>	Paul Fleurat-Lessard, Laboratoire de Chimie, École Normale Supérieure (ENS) de Lyon.

5.3.1 Scientific project

The Human Immunodeficiency Virus (HIV) replicates itself using the human cell machinery as well as its own aspartic protease, so-called HIV-1 PR. The HIV-1 PR is thus essential for the virus maturation, and has become the target for anti-HIV drugs. However, mutants resistant to multi-drug therapies have started to appear. New inhibitors that could efficiently block the HIV-1 PR is a major scientific and human challenge. The chemistry department of the École Normale Supérieure in Lyon is developing a new class of HIV-1 PR inhibitors. In order to design better inhibitors, we are studying the whole enzymatic process using molecular dynamic simulations. This requires the accurate description of the hydrolysis of a peptide bond, as well as the

formation of other bonds. In other words, one must use a quantum description for the reactive part of the protein. However, a quantum description of the whole protein is neither affordable nor needed because the important electronic processes are all located in a small part of the enzyme: the active site which consists of approximately 100 atoms compared to the whole protein (more than 3000 atoms).

5.3.2 Objectives in this Joint Research Activity

The aim of this project is thus to couple an *ab initio* molecular dynamics code (CPMD) with a classical molecular dynamics program (GROMACS) in order to use a hybrid description of the enzymatic process: the reactive centre will be described using Density Functional Theory (DFT) molecular dynamic whereas the rest of the solvated protein will be described by the classical AMBER force field.

We propose a two step procedure:

- The first step will consist in adapting CPMD and GROMACS, as well as developing the coupling between these two codes. A coupling scheme already exists between CPMD and GROMACS. However, it relies on files and is thus far from the efficiency requirements of the DEISA architecture. This new scheme will be tested using standard systems taken for the benchmarks of CPMD and GROMACS, as well as with the previous HIV-1 PR studies.
- The second phase will be the production one: the CPMD / GROMACS code will be used to study the long time dynamics of the HIV-1 PR complexed with standard substrates and with new inhibitors. One point of interest will be to study the link between the slow dynamic of the enzyme and the ease of the chemical reaction. This will allow us to propose inhibitors that will be not only more efficient, but also more resistant to mutations.

In parallel, we would like to improve the coupling scheme in order to have something more flexible. Indeed, the hybrid description is only needed during reactive phases, that is during the phases of the dynamics where bonds are broken or formed. These reactive phases are quite short (some picoseconds) while the non reactive phases are quite long (hundreds of picoseconds, sometimes nanosecond). Our long term goal is thus to use classical molecular dynamics during the non-reactive phase and to dynamically switch to hybrid dynamics (or coupled dynamics) when needed. More, the program will use the hybrid simulations to improve the force field parameters used during the non reactive phases.

6. Conclusion

This document concludes the close collaborations with researcher teams involved in the 3 coupling projects of the second set, in which several major achievements have been done.

From a technical point of view, we were able to run efficiently a large configuration of the Combustion / Radiation project in DECI context, rarely reached in coupled application case. We also performed substantial improvements to the multi-scale/ multi-physics project dealing with aeroelastic phenomena which allow now to tackle more realistic and accurate simulations. This is also the case for the Natural Convection / Radiation project which has benefited, important enhancements which allow today to investigate specific 3D physical configurations not reachable 18 months before.

From a scientific point of view, exploiting the last coupled application releases, developed in this JRA, forms a part of the objectives of the involved research teams. Two PhD thesis planned for the end of 2007 are directly connected with the coupled applications in different scientific domains and with the work realized in the DEISA framework. The scientific and technical efforts carried out in this coupling activity have been recognized by the acceptance of three international scientific publications / communications.

In the next months, HLRS and IDRIS are going to focus on the 3 new projects presented previously and are going to provide a usual support to preceding projects.

7. References and Applicable Documents

- [1] <http://www.deisa.org>
- [2] <http://www.omg.org>
- [3] <http://omniorb.sourceforge.net/>
- [4] <http://unicore.sourceforge.net/>
- [5] <http://www.eurogrid.org/>
- [6] <http://www.limsi.fr/>
- [7] <http://www.let.ensma.fr/>
- [8] <http://www.em2c.ecp.fr/>
- [9] <http://www.em2c.ecp.fr/ACTIVITES/NUMERIQUE/CORAYL/corayl.html>
- [10] <http://www.cerfacs.fr>
- [11] <http://www.cerfacs.fr/~palm>
- [12] Deliverable D-JRA6-1 — *Grid-enabled simulation codes: status report of first release* — October 2004.
- [13] Deliverable D-JRA6-2 — *Production operation of distributed simulation codes: status report* — April 2005.
- [14] Deliverable D-JRA6-3 — *Production operation of distributed simulation codes: status report* — October 2005.
- [15] Deliverable D-JRA6-4 — *Grid enabling the second set of projects: status report of the first release* — April 2006.
- [16] Deliverable D-JRA6-5 — *Production operation of distributed simulation codes: second set of projects* — October 2006.
- [17] M. Lecanu, S. Ducruix, O. Gicquel, E. Iacona, D. Girou, J.M. Dupays and D. Veynante — *Numerical simulation of turbulent combustion including pollutant formation and radiative heat transfers using coupled codes* — Tenth International Conference on Numerical Combustion, Sedona, Arizona, U.S.A on May 9-11 2004 organised by the SIAM (Society for Industrial and Applied Mathematics).
- [18] R. Gonçalves dos Santos, M. Lecanu, S. Ducruix, O. Gicquel, E. Iacona, and D. Veynante, – *Large Eddy Simulations of combustion / radiative heat transfers coupling using the specialized communication language CORBA* – The Cyprus International Symposium on Complex Effects in Large Eddy Simulations (CY-LES 2005) – Limassol, Cyprus (September 2005).

-
- [19] R. Gonçalves dos Santos, S. Ducruix, O. Gicquel, E. Iacona, and D. Veynante — *Large Eddy Simulations of Turbulent Combustion Including Radiative Heat Transfers using Specialized Communication Language* — 11th International Conference on Numerical Combustion, Granada, Spain (2006).
- [20] R. Gonçalves dos Santos, S. Ducruix, O. Gicquel, D. Joseph, M. El Hafi and D. Veynante — *Large Eddy Simulation Including Radiative Heat Transfer* — Third European Combustion Meeting ECM 2007, Chania, Crete (May 2007). Proceedings from the Third European Combustion Meeting 2007.
- [21] R. Gonçalves dos Santos, M. Lecanu, S. Ducruix, O. Gicquel, E. Iacona and D. Veynante — *Coupled Large Eddy Simulations of Turbulent Combustion and Radiative heat transfer* — submitted to *Combustion and Flame* (March 2007).
- [22] R. Gonçalves dos Santos — PhD thesis: « Modélisation et simulation aux grandes échelles de la combustion turbulente avec prise en compte du rayonnement par technique de couplage de code » (*Coupled Large Eddy Simulations of turbulent combustion and radiative heat transfer*) — not definitive title, planned to autumn 2007, EM2C laboratory, Paris, France.
- [23] H. Wang, S. Xin et P. Le Quéré — *Etude numérique du couplage de la convection naturelle avec le rayonnement de surfaces en cavité carrée remplie d'air* — C.R. Mécanique (in French), volume 334, pp 48-57 (2006).
- [24] G. de Gassowski et al — *Bifurcations et solutions multiples en cavité 3D différentiellement chauffée* — C.R. Mécanique 331 (2003) 705-711 (in French).
- [25] J.R. Howell — Application of Monte Carlo to heat transfer problems — *Advances in Heat Transfer*, vol. 5, pp. 1-54 (1992).
- [26] A. Beney — PhD thesis: « *Etude du couplage entre la convection naturelle et le rayonnement dans les grandes structures* » – (*Studies on Natural convection and radiation coupling in large confinements*) — not definitive title (in French), planned to November 2007, EM2C laboratory, Paris, France.
- [27] N. Rouger — PhD thesis — in *preparation*, Laboratoire d'Etudes Thermiques (LET), Poitiers, France.
- [28] H. Klimach, S. P. Roller, J. Uetzmann and C.-D. Munz — *Parallel Coupling of Heterogeneous Domains with KOP3D using PACX-MPI* — Accepted for Presentation on ParCFD 2007 — Antalya, Turkey (May 21-24 2007).
- [29] J.R. Scott — *Single airfoil gust response* — In Proceedings of 4th Computational Aeroacoustics (CAA), Workshop on Benchmark Problems, (September 2004) — NASA/CP-2004-212954.

8. Document Amendment Procedure

9. List of Acronyms and Abbreviations

AVBP	CFD code for numerical simulation of unsteady turbulence for reactive flows (developed by the CERFACS).
CFD	Computational Fluid Dynamics.
CFL	Courant-Friedrichs-Lewy condition. Time step constrain to obtain a correct convergence to solve partial differential equations.
CORBA	Common Object Request Broker Architecture is the OMG's specification which defines the middleware to allow remote computer applications to work together over networks.
DG	Discontinuous Galerkin.
DNS	Direct Numerical Simulation.
DOM	Discrete Ordinate Method.
DFT	Density Functional Theory.
EM2C	Laboratoire d'Energetique Moléculaire et Mascroscopique, Combustion at Chatenay Malabry, France.
FV(M)	Finite Volume (Method).
IAG	Institut für Aerodynamik und Gasdynamik, Stuttgart University, Germany.
LES	Large Eddy Simulation.
LET	Laboratoire d'Etudes Thermiques at Poitiers, France.
LIMSI	Laboratoire d'Informatique pour la Mécanique et les Sciences de l'Ingénieur at Orsay, France.
OMG	The Object Management Group is a consortium that produces and maintains computer industry specifications for interoperable enterprise applications. The other well-known specifications are UML (Unified Modelling Language) and MDA (Model Driven Architecture).
OpenMP	Open Multi Processing.
PACX-MPI	Parallel Computer eXtension MPI.
RMS	Root Mean Square.
RTE	Radiative Transfer Equation.
RHT	Radiative Heat Transfer.